Nanolaminated Permalloy Core for High-Flux, High-Frequency Ultracompact Power Conversion

Jooncheol Kim, Minsoo Kim, Preston Galle, Florian Herrault, *Member, IEEE*, Richard Shafer, Jae Y. Park, *Member, IEEE*, and Mark G. Allen, *Fellow, IEEE*

***Abstract*—Metallic magnetic materials have desirable magnetic properties, including high permeability, and high saturation flux density, when compared with their ferrite counterparts. However, eddy-current losses preclude their use in many switching converter applications, due to the challenge of simultaneously achieving sufficiently thin laminations such that eddy currents are suppressed (e.g., 500 nm–1 μm for megahertz frequencies), while simultaneously achieving overall core thicknesses such that substantial power can be handled. A CMOS-compatible fabrication process based on robot-assisted sequential electrodeposition followed by selective chemical etching has been developed for the realization of a core of substantial overall thickness (tens to hundreds of micrometers) comprised of multiple, stacked permalloy ($Ni_{80}Fe_{20}$) nanolaminations. Tests of toroidal inductors with nanolaminated cores showed negligible eddy-current loss relative to total core loss even at a peak flux density of 0.5 T in the megahertz frequency range. To illustrate the use of these cores, a buck power converter topology is implemented with switching frequencies of 1–2 MHz. Power conversion efficiency greater than 85% with peak operating flux density of 0.3–0.5 T in the core and converter output power level exceeding 5 W was achieved.**

***Index Terms*—Eddy-current loss suppression, high-flux and high-frequency (HFHF) operation, laminated magnetic alloy.**

I. Introduction

THE increasing demand of multifunctional, reduced-size, portable electronic devices is driving the development of miniaturized dc/dc converters [1], [2]. For instance, state-of-the-art smart phones consist of multiple functional blocks such as display panel, MEMS accelerometer, data storage devices, etc, which might require different driving voltages. Miniaturized dc/dc converters could be an effective solution for proper power management of each component.

However, miniaturization of the switching converter cannot be realized without downsizing the passive components, i.e., capacitors and inductors. These passive elements are typically the bulkiest elements in the switcher, and are also challenging to integrate, which impedes the realization of monolithic solutions for power conversion systems [3]. Hence, there have been numerous attempts to increase converter switching frequency into the megahertz range. Such frequency increases reduce the required values of the passive elements [4]. Inductors in particular can be further miniaturized by use of magnetic core materials due to their high permeability [5], [6]. However, incorporation of magnetic core materials can result in frequency-dependent core losses, such as hysteresis and eddy-current losses, within the magnetic material. These losses may limit the power handling capacity and conversion efficiency of the converter. Ferrite materials have been used to reduce eddy-current losses, but the relatively low saturation flux density of these materials limits the operating flux and, therefore, the ultimate achievable degree of miniaturization. Although metallic magnetic materials show superior magnetic performance, eddy-current losses have typically precluded their use at high frequency and high power.

The purpose of this research is to develop a magnetic core material that satisfies the contradictory requirements stated previously. The magnetic material should be able to be operated at high peak flux density (e.g., up to 0.5 T), be capable of being formed into cores with Watt-level power handling capability, and be able to be operated at high frequency (0.5–10 MHz), while simultaneously achieving effective power conversion efficiencies exceeding 80%. In Section II, we have assessed and compared several magnetic materials that are widely utilized as energy storage/transfer components at various operation frequencies. In addition, we have discussed the advantages of highly laminated soft magnetic metallic alloys with respect to other candidate materials, i.e., ferrite and silicon steels, for miniaturized, highly efficient inductive components operating in the 0.5–10 MHz regime. To realize such magnetic material, Section III introduces a CMOS-compatible fabrication process based on automated sequential electrodeposition through a photoresist mold defined by conventional lithography. Section IV provides the magnetic characterization of the material, verifying the suppression of eddy-current losses in the megahertz frequency range, and illustrating its use in a multiwatt dc–dc converter.

II. Magnetic Core Material Consideration

Magnetic materials, e.g., metal alloy [7], [8], ferrites [9], [10], magnetic powders [11], [12], and silicon steels [13] are widely used and researched as electrical energy storage/transfer elements in switched energy conversion. Table I presents typical properties of commercially available magnetic materials as well as newer materials currently under development. Typically,

Manuscript received June 10, 2012; revised September 25, 2012 and December 27, 2012; accepted December 28, 2012. Date of current version February 15, 2013. This work was supported by the Advanced Research Projects Agency-Energy under the Agile Delivery of Electrical Power Technology program (Award DE-AR0000107). Recommended for publication by Associate Editor C. O'Mathuna.

J. Kim, M. Kim, F. Herrault, R. Shafer, and M. G. Allen are with the Department of Electrical and Computer Engineering, Georgia Institute of Technology, Atlanta, GA 30332 USA (e-mail: jkim611@gatech.edu; mkim354@gatech.edu; fh59@mail.gatech.edu; richard.shafer@gatech.edu; mallen@gatech.edu).

P. Galle is with SiTime Corporation, Sunnyvale, CA 94085 USA (e-mail: wpgalle3@gmail.com).

J. Y. Park is with the Department of Electronic Engineering, Kwangwoon University, Seoul 139-701, Korea (e-mail: jaepark@kw.ac.kr).

Color versions of one or more of the figures in this paper are available online at http://ieeexplore.ieee.org.

Digital Object Identifier 10.1109/TPEL.2013.2238639

0885-8993/$31.00 © 2013 IEEE

TABLE I
PROPERTIES OF DIFFERENT TYPES OF MAGNETIC MATERIALS

Magnetic Materials	B_S [T]	H_C [Oe]	μ_r	ρ [Ω·m]	Lamination Thickness [μm]
Laminated Permalloy (100layer) (This Work)	1.2	1.5	300	3e-8	0.5
Co-Zr [17]	1	1	100	3E-6	0.1
CoZrTa [18]	1.52	0.015	1000	1E-6	0.5
CoFeO [19]	1.05	5	200	2.2E-5	0.006
Ferrite [20] (4F1 from Ferroxcube)	0.32	2	80	1e6	800
Ferrite [21] (67 TOROID from Fari Rite)	0.23	3.5	40	1e6	1650
Fe-Si [22] (AK M-47 from DI-MAX)	2.08	0.57	6800	37e-8	1650

ferrites are commonly used for high-frequency power electronic applications due to their inherent low electrical conductivity, resulting in negligible eddy-current loss at high frequency (>1 MHz). However, typical ferrites possess low saturation flux densities and permeabilities, making it challenging to miniaturize these magnetic components if they must carry significant amounts of power; thus, it is often true that magnetic components are the physically largest single elements in power conversion systems. Also, the high sintering temperature of ferrite impedes CMOS-compatible integration of magnetic components on a single chip for ultracompact converter applications. To attempt to overcome these limitations of ferrites, magnetic metallic alloys, including NiFe, CoZr, and CoNiFe, have been arisen as attractive alternatives. These materials have higher saturation flux densities and permeabilities, as well as higher thermal conductivities, potentially enabling further miniaturization of total core volume in magnetic components. However, the typical drawback of the metallic alloys is still linked to their low electrical resistivity, which can lead to substantial eddy-current loss in the core at high-frequency operation [14]–[16]. In order to utilize these nonzero conductivity (i.e., finite skin depth) metallic alloys, therefore, a method for laminating these films, with lamination thicknesses less than the skin depth, is required. Two methods to achieve laminations of the appropriate thickness are available: increasing the electrical resistivity of the material to increase the needed lamination thickness; or decrease the lamination thickness achievable through fabrication advances. For example, commercially available Si–Fe laminations have larger resistivities than permalloy; however, they still normally allow significant eddy-current loss beyond 1 kHz operation frequency due to the technical difficulties of fabricating thin (<50 μm) steel sheet by conventional means. Recently, researchers have demonstrated nanolaminated sputtered magnetic alloys with remarkable high-frequency characteristics [17]–[19]. However, those alloys are not yet widely available with overall (i.e., sum of lamination layers) thicknesses beyond tens of micrometers; yet, significant overall thickness is required for power handling capability in the tens of watts range and above. In order to simultaneously achieve thin laminations sufficient to suppress eddy-current loss as well as overall thicknesses allowing power handling in the tens of watts and beyond, we developed nanolaminated permalloy cores with single-layer thicknesses precisely controlled well below the skin depth (1–2 μm) of the material even at 10 MHz, while the overall thickness exceeds tens of micrometers. This approach is an effective way to maintain the superior magnetic properties (i.e., higher saturation flux density and permeability) of metallic alloys as well as achieve sufficiently large magnetic material volume to handle large amounts of magnetic energy.

III. FABRICATION OF A NANOLAMINATED PERMALLOY CORE

The fabrication process for the nanolaminated permalloy core is based on automated sequential electrodeposition of ferromagnetic permalloy and sacrificial material [see Fig. 1(a)], followed by selective removal of the sacrificial layers so as to insulate each permalloy layer [see Fig. 1(b)]. Copper was chosen for the sacrificial material as it exhibits low surface roughness, high adhesion to the magnetic material, and is able to be selectively etched away without degrading or etching the magnetic material [23].

The fabrication starts with forming a thick photoresist mold on top of a sputtered metallic seed layer (titanium/copper/titanium). After the pre-electrodeposition sample preparation (i.e., titanium etching and copper deoxidation), the mold is filled with alternating layers of ferromagnetic permalloy and copper using the robotic multilayer electrodeposition system [see Fig. 1(c)]. The total thickness of the sequential electro deposition is linked to the thickness of the mold, which typically can vary from tens of micrometers to the millimeter-scale depending on the targeted thickness of the core. A Watts-type bath was employed for the electrodeposition of permalloy [24], and a commercial copper bath (*Grobet, Clean Earth Cu-mirror solution*) containing brighteners and levelers was utilized for copper electrodeposition. The multilayer deposition system is based on a robotic arm which moves the sample from one bath to another. The robot-assisted system allows the fabrication of hundreds of layers with precisely controlled individual layer thickness, which is a significant improvement compared to the previous work done by manual multilayer electrodeposition [25]. After the photoresist mold is removed by acetone, a short selective copper wet etch is performed to create lateral "grooves" around the sidewall of the structure [see Fig. 1(d)]. This etchant provides excellent selectivity between a magnetic layer and copper. SU-8 epoxy is then applied through the "etch holes" depicted in Fig. 1(e), which refer to the areas that were covered by the plating mold during the electrodeposition. A subsequent UV exposure and postexposure bake allows us to leave a portion

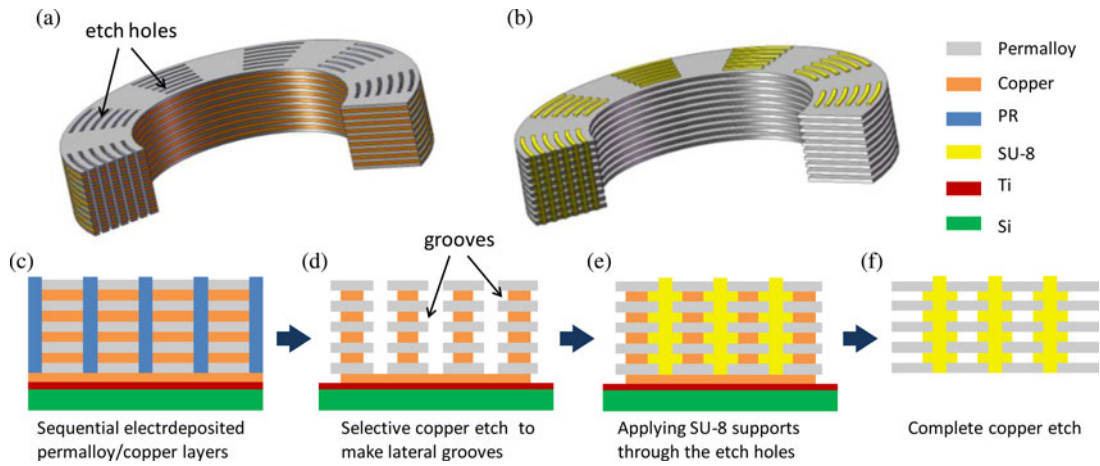

Fig. 1. Fabrication process for the nanolaminated permalloy core. (a) Schematic of electrodeposited multilayers (eddy currents are dominant). (b) Schematic of the laminated metal/insulator structure (eddy currents are suppressed). (c)–(f) Detailed sequence for the fabrication of the nanolaminated permalloy core.

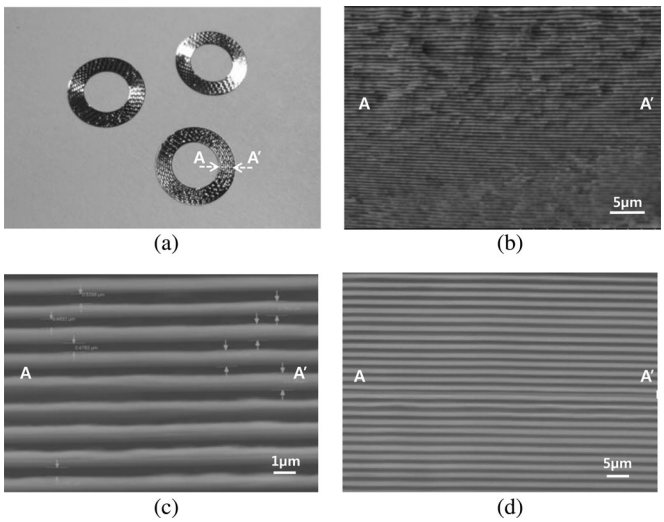

Fig. 2. Images of the nanolaminated permalloy core. (a) Toroidal type permalloy cores. (b) Cross section of a core with 100 layers of 500 nm permalloy layers. (c) Magnified cross-sectional view of 500–nm-thick layers. (d) Cross section of a core with 1 μm layers.

of "etch holes" filled with cross-linked SU-8 [see Fig. 1(e)]. Next, the sacrificial copper layers are completely removed in the etchant through the periphery of the structure and the "etch holes" unoccupied by SU-8 so that individual laminations can be created [Fig. 1(f)]. Note that the nonconductive SU-8 filled in the "grooves" as well as in the etch holes allows the permalloy layers to maintain their mechanical integrity after the copper removal, in comparison to the previous work where an additional electrodeposition of conductive structures was employed for the same purpose [25]. Through this proposed approach, the complete electrical insulation between permalloy layers is feasible, minimizing the source of eddy-current losses.

To assess the properties of the nanolaminated permalloy, magnetic cores for measurement of eddy-current losses were fabricated with lamination thicknesses ranging from 500 nm to 1 μm, and lamination count up to 100. Fig. 2(a) shows optical images of toroidal shaped cores comprised of 100 layers of permalloy. Note that the dimensions of the cores are precisely determined in a batch scale, due to the use of photolithography.

From the cross-sectional view, we can observe uniform permalloy layers of 500-nm thickness after the selective etching of sacrificial copper layers [see Fig. 2(b) and (c)]. Also, cores with varying numbers of total layers with targeted lamination thickness could be manufactured by a simple adjustment of plating variables. As an example, a cross-sectional view of a laminated structure comprised of 1-μm-thick permalloy layers is shown in Fig. 2(d).

IV. Characterization of a Nanolaminated Permalloy Core

Test inductors are fabricated by packaging nanolaminated permalloy cores in laser-micromachined polymeric bobbins and winding them with low-loss Litz wire. For the fabrication of a bobbin, the polymeric sheet is first laser-scribed to form a toroidal trench at the center where the magnetic core can be securely placed. The trench is slightly deeper than the core thickness and wider than the core outer diameter so that the released core structure does not collapse by subsequent manual coil winding. Then, a number of notches are cut along the periphery of the trench to provide space for tight and reproducible winding without overlap. Fig. 3 shows fabricated inductors with laminated permalloy cores packaged in polymer bobbins, wound by Litz wire having either 36 or 48 turns.

For all measurement results in this paper, a premeasured inductance and resistance of an air core inductor of nominally identical geometry to the inductor of interest, but lacking a magnetic material core, was determined. This was achieved by utilizing the same bobbin geometry wrapped with the same number of turns but with no magnetic core within the bobbin. This premeasured air-core inductance and resistance was subtracted from the inductance and resistance of the inductors with magnetic cores so that the presented results in this paper are attributable to the core material alone.

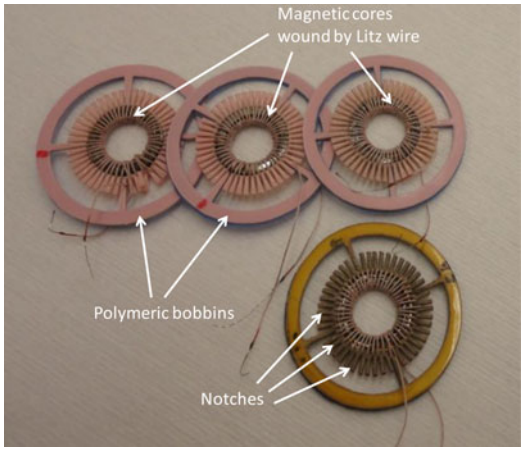

Fig. 3. Fabricated inductors via packaging the magnetic cores in laser-machined polymeric bobbins winding with Litz wire.

A. In Situ Characterization of Nanolaminated Permalloy Cores

Suppression of eddy-current core losses was observed *in situ* during the lamination isolation etch process by measuring frequency-dependent core inductance. For the *in situ* measurement, laminated permalloy cores are packaged in the laser-micromachined bobbins prior to etching and wound with Litz wire. Then, measuring the electrical characteristics (i.e., inductance L and quality factor Q) of the wound inductors allows determination of energy storage and loss in the permalloy core. The measurements were taken prior to sacrificial layer etching, and subsequently at various times during the progression of the sacrificial layer etch, enabling assessment of the eddy-current suppression. The performance of the wound inductors at various stages of lamination etching is assessed by removing the inductors from the etchant, immersing them in deionized (DI) water, measuring their electrical characteristics using an impedance analyzer (HP 4194 A), and returning them to the etch solution for continued etching.

An example of the *in situ* measurements is illustrated in Fig. 4(a). A core consisting of 40 layers of 1-μm-thick permalloy, with each permalloy layer separated by a 1-μm-thick sacrificial copper layer, is wrapped with 36 turns of Litz wire. Before the etching of the sacrificial material ($t = 0$ h), the core is simply a bulk metallic composite, with thickness far exceeding the skin depth in the megahertz range. As a result, a decrease of inductance as a function of frequency can be observed due to the presence of significant eddy-current loss. However, as the copper is being selectively removed in the etchant ($t = 1$–39 h), the frequency-dependent inductance decrease becomes progressively less severe, indicating reduction in the eddy-current effect. After $t = 39$ h, no inductance variation with frequency is observed. These measurements not only directly validate our strategy toward eddy-current suppression, but also provide an efficient way of verifying the complete removal of sacrificial layers. Upon removal of the sacrificial copper, the core was immersed in isopropanol, and rapidly dried in an oven. The quality factor of the dried device reaches as high as 60 at a frequency of 1 MHz as shown in Fig. 4(b), implying there is little inter-

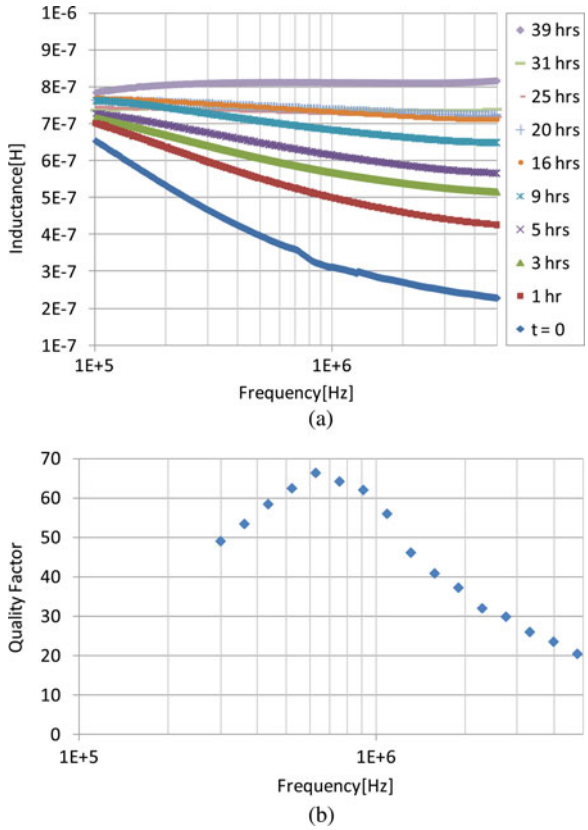

Fig. 4. (a) Inductance change of the packaged inductor with respect to the etch time of the sacrificial layers ($t = 0$–39 h). Individual low-frequency inductances are subject to compensation errors, but the frequency dependence of the inductance clearly shows the beneficial effect of interlamination conductor removal. (b) Core quality factor reaching as high as 60 at 1 MHz.

layer electrical conduction upon completion of the fabrication process.

B. High-Flux, High-Frequency (HFHF) Performance of the Nanolaminated Permalloy Core

Nanolaminated permalloy cores enable the fabrication of inductors operating in the megahertz frequency range with exceptionally high operating flux density of 0.5 T, which is hardly achievable with conventional ferrite or the soft magnetic thin films [9]–[11], [25]. In order to characterize the superior performance of the nanolaminated permalloy cores, HFHF core-loss measurements were performed using an *LC* resonant test setup based on series resonance between the inductor under test and a reference capacitor [26]. A circuit diagram of the HFHF core-loss characterization setup is shown in Fig. 5. The inductor is modeled as a series connection of an ideal inductor with inductance of L and two resistive components ($R_{\rm cu}, R_{\rm core}$). $R_{\rm cu}$ and $R_{\rm core}$ represent the copper and core losses of the inductor, respectively. R_c and C represent a capacitor, which is selected to resonate with the inductor at the desired measurement frequency. A sinusoidal voltage $V_{\rm in}$ is generated by an RF power source, which is comprised of a signal generator and an amplifier. By tuning the amplitude and the frequency of $V_{\rm in}$, the excitation of the circuit is modulated, and therefore, the flux density within the core is controlled.

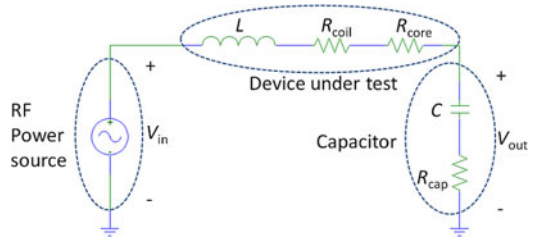

Fig. 5. Schematic of the HFHF core-loss characterization setup.

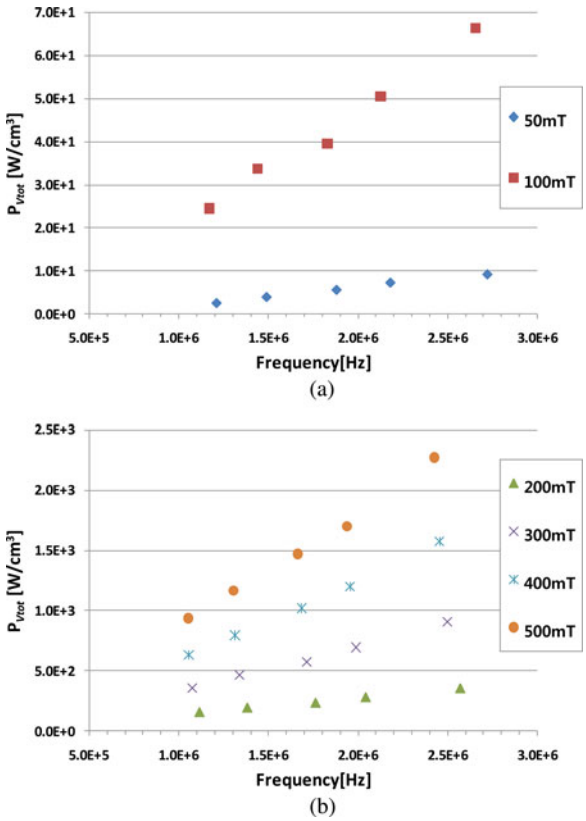

Fig. 6. Measured power loss per unit volume up to 0.5 T flux density at low megahertz frequency. Data are shown in two plots to delineate low and high flux operation: (a) 0.05 T and 0.1 T, (b) 0.2–0.5 T.

The voltages $V_{\rm in}$ and $V_{\rm out}$ are monitored by an oscilloscope. The measured value of $V_{\rm in}$, together with the premeasured printed circuit board/capacitor impedance, is used to calculate the current and power dissipation in the circuit. An additional probe is connected to the secondary pickup coil of the inductor to directly extract the voltage so that the flux within the core can be calculated using Faraday's law of induction.

To measure the inductor losses, the *LC* circuit is operated at its resonant frequency. At this frequency, the *LC* circuit acts as a purely resistive load, which allows the calculation of its power dissipation as the product of the root-mean-square values of the *LC* circuit's current and measured voltage waveforms $(V_{\rm in}, V_{\rm out})$.

Fig. 6 shows measured volumetric power loss up to 0.5-T flux density in the 1–3 MHz frequency range from a 40 layer permalloy core with 500-nm lamination thickness, indicating that the nanolaminated permalloy core inductor operates at high

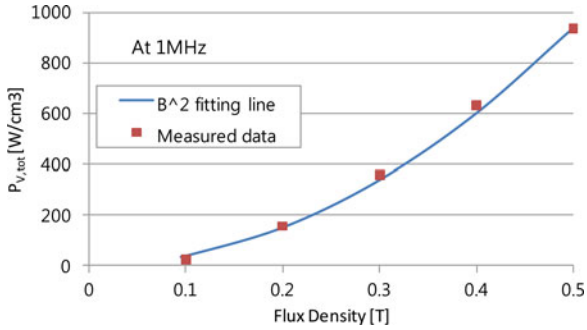

Fig. 7. Measured power loss per unit volume at 1 MHz as a function of flux density.

flux with reasonable volumetric power. For comparison, the laminated core at an operating magnetic field of 0.1 T and 2 MHz shows a total loss of 48 W/cm^3, which is lower than that of commercial ferrite from Ferroxcube [20]. The total power loss of the commercial ferrite at the same operating flux and frequency is estimated to be 60 W/cm^3 using the Steinmetz equation [2].

Although the operation of the nanolaminated permalloy cores at high flux densities up to 0.5 T will lead to increasing core loss and, therefore, increasing heat generation, the high thermal conductivity of the core coupled with the relatively high surface-to-volume ratio of the core facilitates heat transfer from the core in a manner superior to the lower thermally conducting ferrites. In order to monitor the temperature variation of the nanolaminated permalloy core in high flux density operation, the core temperature has been measured using an infrared thermometer during the HFHF core-loss measurement. Negligible temperature change of the core was observed at operation up to 0.2 T flux density without any thermal cooling, demonstrating the high heat dissipation capability of the core. However, some type of thermal management ranging from heat sinking to convective cooling may be required in higher flux operation; in the measurements performed here, convective cooling of a nonheat-sunk inductor was employed at the highest fluxes. Further improvements of the loss figures of the nanolaminated permalloy can be achieved by focusing efforts on reduction of hysteresis loss; even with its current loss figures, the material can be utilized at higher magnetic fluxes up to 0.5 T.

In order to estimate a correlation between flux density and nanolaminated permalloy core loss, flux-dependent volumetric power loss of the nanolaminated permalloy core is plotted as a function of flux B, with a B^2 fitting line for reference as shown in Fig. 7. The measured data points at 1 MHz demonstrate that the volumetric power loss increase of this magnetic material correlates with B^2 as expected.

C. Hysteresis Loss and Eddy-Current Loss of Nanolaminated Permalloy Cores

In order to verify suppression of eddy-current losses of a nanolaminated permalloy core at high flux density, it is required to distinguish eddy-current losses and hysteresis losses from the total power losses. The distribution of electric fields, magnetic fields, and eddy currents in the magnetic core can be analytically modeled for a rectangular lamination [14], [15], decomposing

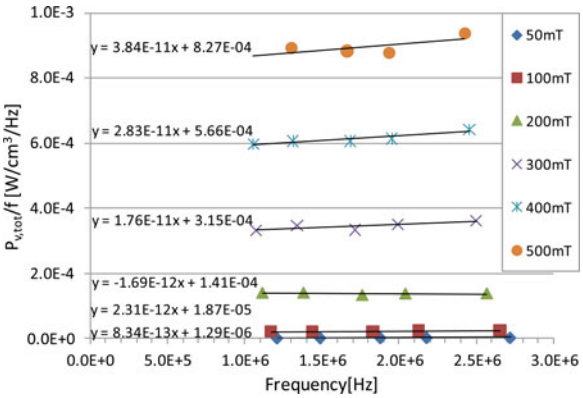

Fig. 8. Measured power loss per unit volume over operation frequency up to 0.5-T flux density.

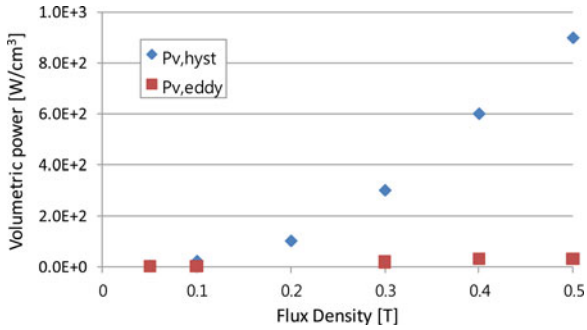

Fig. 9. Comparison of eddy-current loss with hysteresis loss at 1 MHz as a function of flux density.

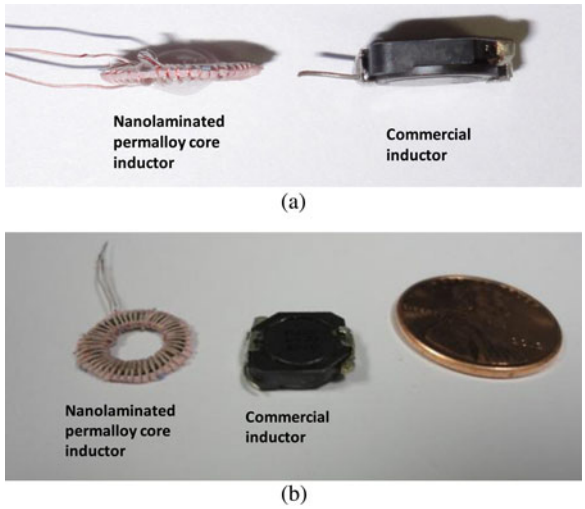

Fig. 10. Comparison of commercial inductor and a laminated permalloy core inductor with penny. Both inductance values are approximately 1 μH. (a) Side view of both inductors. (b) Inclined top view of both inductors with penny.

the total volumetric power loss across the core $P_{V,\mathrm{tot}}$ into volumetric eddy-current loss $P_{V,\mathrm{eddy}}$ and hysteresis loss $P_{V,\mathrm{hyst}}$ depending on the lamination thickness. A thin approach does not specifically resolve proximity and anomalous loss; instead, they are lumped into hysteresis and eddy-current losses. For the cores with lamination thickness below the skin depth, both eddy-current and hysteresis losses become a function of frequency-squared and frequency, respectively

$$P_{V,\mathrm{eddy}} \propto f\left(\frac{a}{\delta}\right)^2 \propto \omega^2 \text{ and } P_{V,\mathrm{hyst}} \propto f \propto \omega \qquad (1)$$

where a is the lamination thickness and δ is the skin depth.

This analytical modeling shows that eddy-current losses and hysteresis losses are distinguishable from each other in the thin lamination regime where the lamination thickness is well below the skin depth by analyzing the core losses as a function of frequency. Given the relative permeability and resistivity of permalloy [25], the skin depth at 1 MHz is at least 10 μm which is much thicker than the fabricated lamination thickness of 0.5–1 μm.

As a result, total loss per unit volume $P_{V,\mathrm{tot}}$ of a nanolaminated permalloy core can be written as

$$P_{V,\mathrm{tot}} = P_{V,\mathrm{eddy}} + P_{V,\mathrm{hyst}} = k_{\mathrm{eddy}} f^2 + k_{\mathrm{hyst}} f \qquad (2)$$

where k_{eddy} is defined as the eddy-current power loss density coefficient and k_{hyst} is defined as the hysteresis power loss density coefficient.

Consequently, by plotting $P_{V,\mathrm{tot}}$/frequency as a function of frequency, the coefficients k_{eddy} and k_{hyst} can be extracted from the graph's slope and intercept, respectively. Measured volumetric power losses up to 0.5-T flux density in the 1–3 MHz frequency range from a 40 layer permalloy core with 500-nm lamination thickness are plotted in Fig. 8, and linear fits are extracted from the measured data points for each flux density. The negative slopes are interpreted as a measurement resolution limitation, indicating that the eddy-current losses are so small compared to the hysteresis losses that it was not possible to resolve them at these frequencies. Fig. 9 shows the volumetric power for both eddy-current and hysteresis losses at 1 MHz as a function of peak flux density. It demonstrates that the eddy-current losses are suppressed to negligible levels compared to the magnitude of the hysteresis losses.

D. Performance of the Nanolaminated Permalloy Core in a Buck Converter

The fabricated inductor with nanolaminated permalloy core has been tested in a buck power converter with switching frequencies in the megahertz range. The LM3103 evaluation board from Texas Instruments (TI) was selected in order to demonstrate power converter performance of the inductor. This board is designed as a step-down switching regulator, which is operating as a buck power converter. A diagram of the evaluation board as well as typical component values can be found in [27]. The typical switching frequency of the power converter is approximately 0.5 MHz. By modifying the resistor that sets the switching frequency, and by replacing the commercial inductor by low-profile, 36-turn inductor with 40 layer permalloy core with 1-μm lamination thickness, the converter operates switching frequencies above 1 MHz with power output levels above 5 W and efficiencies greater than 85%.

Fig. 10 shows an image of a commercial inductor and the nanolaminated permalloy core inductor of similar inductance value of 1 μH. For comparison, the volume of the nanolaminated permalloy core inductor even including nonoptimized Litz wire winding is approximately 90 mm^3, whereas the packaged commercial inductor volume measured 260 mm^3, indicating

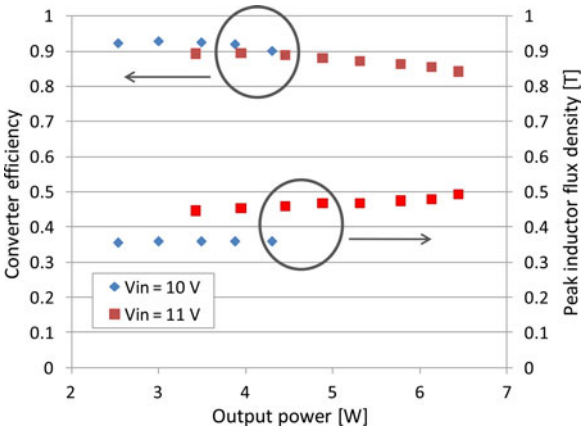

Fig. 11. Experimental measurements of power converter performance tested with a nanolaminated permalloy core inductor. Power converter efficiency and peak inductor flux density as a function of output power.

the large inductor size reduction enabled by the nanolaminated magnetic core technology. The smaller volume of the nanolaminated permalloy core is mainly due to the higher saturation flux density and permeability of the magnetic material. Greater power density can be achieved with the nanolaminated permalloy core since the operating flux density can be higher than that of commercial ferrite. The volume of the nanolaminated permalloy core itself is 1.5 mm^3.

Fig. 11 shows experimental measurements of the power converter performance operated with the nanolaminated permalloy core inductor, demonstrating 87% efficiency with output power of 5 W at 1.25 MHz. The peak inductor flux density was also calculated by measuring the inductor current. Exploiting the high saturation flux density of the nanolaminated inductor, a substantially smaller magnetic volume of core is utilized, compared to the commercial inductor. The nanolaminated inductor operates at very high fluxes (0.3–0.5 T) while maintaining system efficiencies of 85% and above. For comparison, typical commercial inductors are operated at approximately 0.02–0.04 T of peak inductor flux density in order to maintain high efficiencies.

V. Conclusion

We designed and fabricated a nanolaminated permalloy core. The core fabrication procedure is comprised of CMOS-compatible processes with minimal use of vacuum tools, providing potential for the batch production of miniaturized ultrahigh-power on-chip devices. The presented nanolaminated permalloy core is demonstrated to operate in the MHz range without suffering from eddy-current losses. Also, the large magnetic volume enabled by the large number of thin laminations, together with the high magnetic flux density of the material, enables magnetic components with operating flux density up to 0.2 T with negligible temperature rise, and 0.5 T, which are relatively small volume cores that can be operated in relatively large power applications. Negligible core temperature increases were observed at operating flux densities of 0.2 T, and operation up to 0.5 T was achieved with appropriate thermal management. The nanolaminated permalloy cores were utilized in a power converter (TI LM3013 switcher) demonstrating 87% efficiency with output power of 5 W at 1.25 MHz. The increasing noneddy-current losses (i.e., hysteresis losses and thermal losses) at high operation flux densities can be further reduced mainly by utilizing low coercivity ferromagnetic materials, which is under current investigation.

Acknowledgment

Microfabrication was carried out in part in the Georgia Tech's Institute for Electronics and Nanotechnology. Donation of evaluation boards from Texas Instruments is gratefully acknowledged.

References

[1] R. J. Huljak, V. J. Thottuvelil, A. J. Marsh, and B. A. Miller, "Where are power supplies headed?" in *Proc. 15th Annu. IEEE Appl. Power Electron. Conf. Expo*., Feb. 6–10, 2000, vol. 1, pp. 10–17.

[2] S. C. O. Mathuna, T. O'Donnell, N. Wang, and K. Rinne, "Magnetics on silicon: An enabling technology for power supply on chip," *IEEE Trans. Power Electron*., vol. 20, no. 3, pp. 585–592, May 2005.

[3] A. W. Lotfi and M. A. Wilkowski, "Issues and advances in high-frequency magnetics for switching power supplies," *Proc. IEEE*, vol. 89, no. 6, pp. 833–845, Jun. 2001.

[4] N. Wang, T. O'Donnell, S. Roy, P. McCloskey, and C. O'Mathuna, "Microinductors integrated on silicon for power supply on chip," *J. Magn. Magn. Mater.*, vol. 316, no. 2, pp. e233–e237, Sep. 2007.

[5] D. Flynn, A. Toon, L. Allen, R. Dhariwal, and M. P. Y. Desmulliez, "Charaterization of core materials for microscale magnetic components operating in the megahertz frequency range," *IEEE Trans. Magn*., vol. 43, no. 6, pp. 3171–3180, Jul. 2007.

[6] C. O'Mathuna, N. Wang, S. Kulkarni, and S. Roy, "Review of integrated magnetic for power supply on chip (PwrSoC)," *IEEE Trans. Power Electron*., vol. 27, no. 11, pp. 4799–4816, Nov. 2011.

[7] T. Osaka, M. Takai, K. Hayashi, K. Ohashi, M. Saito, and K. Yamada, "A soft magnetic CoNiFe film with high saturation magnetic flux density and low coercivity," *Nature Mater*, vol. 392, no. 23, pp. 796–798, Apr. 1998.

[8] S. Ohnuma, H. J. Lee, N. Kobayashi, H. Fujimori, and T. Masumoto, "Co-Zr-O nano-granular thin films with improved high frequency soft magnetic properties," *IEEE Trans. Magn*., vol. 37, no. 4, pp. 2251–2254, Jul. 2001.

[9] H. Jia, J. Lu, X. Wang, K. Padmanabhan, and Z. J. Shen, "Integration of a monolithic buck converter power IC and bondwire inductors with ferrite epoxy glob cores," *IEEE Trans. Power Electron*., vol. 26, no. 6, pp. 1627–1630, Jun. 2011.

[10] S. Bae, Y.-K. Hong, J.-J. Lee, J. Jalli, G. S. Abo, A. Lyle, B. C. Choi, and G. W. Donohoe, "High Q Ni-Zn-Cu ferrite inductor for on-chip power module," *IEEE Trans. Magn*., vol. 45, no. 10, pp. 4773–4776, Oct. 2009.

[11] M. Wang, J. Li, K. D. T. Ngo, and H. Xie, "A surface-mountable microfabricated power inductor in silicon for ultracompact power supplies," *IEEE Trans. Power Electron*., vol. 26, no. 5, pp. 1310–1315, May 2011.

[12] Y. Zhao, X. Zhang, and J. Q. Xiao, "Submicrometer laminated Fe/SiO_2 soft magnetic composites—an effective route to materials for high-frequency application," *Adv. Mater.*, vol. 17, no. 7, pp. 915–918, Apr. 2005.

[13] T. Takada, M. Abe, S. Masuda, and J. Inagaki, "Commercial scale production of Fe6.5 wt.% Si sheet and its magnetic properties," *J. Appl. Phys*., vol. 64, pp. 5367–5369, Nov. 1988.

[14] G. Bertotti, *Hysteresis in Magnetism*. London, U.K.: Academic, 1998.

[15] J. P. Barranger, "Hysteresis and eddy-current losses of a transformer lamination viewed as an application of the Poynting theorem," in NASA, Washington, DC, USA, NASA TN D-3114, 1965

[16] J. Lammeraner and M. Stafl, *Eddy Current*. London, U.K.: Iliffe, 1966.

[17] J. Qiu and C. R. Sullivan, "Design and fabrication of VHF tapped power inductors using nanogranular magnetic films," *IEEE Trans. Power Electron*., vol. 27, no. 12, pp. 4965–4975, Dec. 2011.

[18] W. Xu, H. Wu, D. S. Gardner, S. Sinha, T. Dastagir, B. Bakkaloglu, Y. Cao, and H. Yu, "Sub-100 μm scale on-chip inductors with CoZrTa for GHz applications," *J. Appl. Phys*., vol. 109, pp. 07A316-1–07A316-3, 1988.

[19] K. Ikeda, K. Kobayashi, and M. Fujimoto, "Multilayer nanogranular magnetic thin films for GHz application," *J. Appl. Phys*., vol. 92, pp. 5395–5400, Nov. 2002.

[20] (2008). [Online]. Available: http://www.ferroxcube.com/prod/assets/4f1.pdf
[21] (2010). [Online]. Available: http://www.mouser.com/catalog/specsheets/5967000201.pdf
[22] (2007). [Online]. Available: http://www.aksteel.com/pdf/markets_products/electrical/Non_Oriented_Bulletin.pdf
[23] F. Herrault, W. P. Galle, R. H. Shafer, and M. G. Allen, "Electroplating-based approaches for volumetric nanomanufacturing," in *Proc. Tech. Dig. Technol. Future Micro-Nano Manuf.*, 2011, pp. 71–74.
[24] J. Y. Park, "Packaging-compatible micromachined magnetic devices: Integrated passive components and modules," Ph.D. dissertation, Dept. Electr. Comput. Eng., Georgia Institute of Technology, Atlanta, GA, USA, Dec. 1997.
[25] J. W. Park, "Core lamination technology for micromachined power inductive components," Ph.D. dissertation, Dept. Electr. Comput. Eng., Georgia Institute of Technology, Atlanta, GA, USA, Dec. 2003.
[26] Y. Han, G. Cheung, A. Li, C. R. Sullivan, and D. J. Perreault, "Evaluation of magnetic materials for very high frequency power applications," in *Proc. IEEE Power Electron. Spec. Conf.*, Jun. 2008, pp. 4270–4276.
[27] (2009). [Online]. Available: http://www.ti.com/lit/ds/symlink/lm3103.pdf

Jooncheol Kim received the B.S. degree in electrical engineering from the Soongsil University, Seoul, Korea, in 2009, and the M.S. degree in electrical and computer engineering from the Georgia Institute of Technology, Atlanta, GA, USA, in 2011. In 2010, he joined the research group of Prof. M. G. Allen, Georgia Institute of Technology, where he is currently working toward the Ph.D. degree in electrical and computer engineering.

His current research interests include fabrication of dissolvable microneedles for transdermal drug delivery and developing high-performance magnetic materials for power supply on a chip.

Minsoo Kim received the B.S. and M.S. degrees in electrical and computer engineering from Seoul National University, Seoul, Korea, in 2006 and 2008, respectively. Since 2010, he has been working toward the Ph.D. degree at the Georgia Institute of Technology, Atlanta, GA, USA.

Until 2009, he was at the Korea Institute of Industrial Technology, where he was involved in the research on inkjet-printed electronics. His current research interests include 3-D microfabrication technology based on multilayer electrodeposition for the realization of a variety of passive and active devices.

Preston Galle received the B.S. degree in electrical engineering from Texas A&M University, College Station, TX, USA, in 1997, and the Ph.D. degree in electrical engineering from the Georgia Institute of Technology, Atlanta, GA, USA, in 2013.

He is currently a Characterization Engineer at SiTime Corporation, Sunnyvale, CA, USA. His graduate work and all associated publications were focused on the microfabrication of magnetic components for energy storage and conversion, especially inductors. Prior to his graduate studies, he was a Hardware Development Engineer for several companies in Portland, OR, USA.

Dr. Galle received the National Defense Science and Engineering Graduate Fellowship Award in 2005 and the National Science Foundation Integrative Graduate Education and Research Training Fellowship Award in 2007.

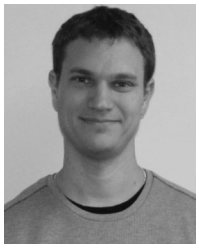

Florian Herrault (M'12) received the B.S. and M.S. degrees in physics and materials science, and the Ph.D. degree in electrical and electronics engineering from the National Institute of Applied Sciences, Toulouse, France, in 2003, 2005, and 2009, respectively.

He is currently a Research Engineer with the MicroSensors and MicroActuators Group, Georgia Institute of Technology, GA, USA. His current research interests include piezoelectric and electromagnetic sensors and actuators, small-scale power generation systems, high-performance magnetics for on-chip power converters, 3-D microelectromechanical systems (MEMS) fabrication, and MEMS-enabled thermal management devices.

Dr. Herrault has been a Member of the technical program committees of the PowerSoc 2010, PowerSoc 2012 International Workshop, and PowerMEMS 2012.

Richard Shafer attended the University of Kentucky majoring in electrical engineering.

He has over twenty years of significant technical experience in diverse research and manufacturing environments. He has a broad technical background with particular expertise in analysis, characterization, processing and fabrication of ceramic materials, and refractory metals, vacuum technology, electrical, electronic and mechanical design, and automation. He was employed in the vacuum tube industry for over 15 years and has knowledge of process procedures, lab procedures, microscopy—both electron and optical, and vacuum systems. He has extensive knowledge in the design, production, and testing of thermionic emitters. As acting laboratory Manager for the MEMS group in Georgia Tech, he maintains the labs and provides support for the people using them.

Jae Y. Park (M'95) received the M.S.E.E. and Ph.D. degrees in electrical and computer engineering from the Georgia Institute of Technology, Atlanta, GA, USA, in 1995 and 1997, respectively.

After graduation, he was at the Georgia Institute of Technology as a Research Engineer for two years. He was in the Microsystem Group, LG Electronics Institute of Technology, as a Team leader of RF microelectromechanical system (MEMS) research for six years. In September 2004, he joined as a faculty member in the Department of Electronics Engineering, Kwangwoon University, Seoul, Korea. He has published more than 180 journal articles and conference proceedings and filed more than 95 patents. His current research interests include microelectromechanical systems (MEMS, microactuators for optical and RF applications), microsystem packaging (wafer-level packaging, microsolders, printed circuit board embedded passives and modules, and system on packaging), nonenzymatic electrochemical sensors, energy harvesting devices and modules, and RF MEMS components and circuits

Mark G. Allen (M'88–SM'04–F'11) received the B.A. degree in chemistry, the B.S.E. degree in chemical engineering, and the B.S.E. degree in electrical engineering from the University of Pennsylvania, Philadelphia, PA, USA, and the S.M. and Ph.D. degrees from the Massachusetts Institute of Technology, Cambridge, MA, USA, in 1989.

Since 1989, he has been with the faculty of the School of Electrical and Computer Engineering, Georgia Institute of Technology, Atlanta, GA, USA, where he is currently a Regents' Professor and the J. M. Pettit Professorship in microelectronics, as well as holds a joint appointment in the School of Chemical and Biomolecular Engineering. His research interests include the development and the application of new micro- and nanofabrication technologies, as well as microelectromechanical system (MEMS).

Dr. Allen is the Editor-in-Chief of the *Journal of Micromechanics and Microengineering*, and was a previous Cochair of the IEEE/ASME MEMS Conference.